PERGAMON

International Journal of Heat and Mass Transfer 44 (2001) 4027–4034

International Journal of
HEAT and MASS
TRANSFER

www.elsevier.com/locate/ijhmt

Determination of temperature in glass with a fluorescence method

C.L. Shepard, B.D. Cannon, M.A. Khaleel *

Engineering Mechanics Group, Pacific Northwest National Laboratory, P.O. Box 999, K2-18, Richland, WA 99352, USA

Received 11 July 2000; received in revised form 9 January 2001

Abstract

We have developed a method for measurement of temperature in glass products with the following features: (1) non-contacting, (2) real time, and (3) through-thickness. The method is based on fluorescence emission. Many glass products include Fe_2O_3 as an additive in various amounts. Ferric (Fe^{3+}) and ferrous (Fe^{2+}) ions absorb light in the ultraviolet and infrared parts of the spectrum. Absorption of light by iron ions in glass results in a predictable fluorescence emission. The emission in turn depends on the glass temperature, and this dependence is the basis for our method of measuring temperature. We have measured the fluorescence emission lifetimes in several commercial automotive glass samples over a temperature range from 25°C to 550°C (about 300–825 K). Imaging the fluorescence emission from glass samples onto a segmented photomultiplier tube provided spatially resolved measurements. A simple model that relates the temperature to the fluorescence lifetime has been developed. Published by Elsevier Science Ltd.

1. Introduction

The measurement of temperature within glass products is of interest to the glass industry for reasons of quality control and process optimization. The efficient production of glass requires that the glass be at certain temperatures during different stages of the production line. The final properties of the glass product depend in part upon the processing temperatures. In the automotive industry, forming of glass can only be properly done when the glass is within a certain temperature range. In the case of tempered products, which accounts for most of the glass within an automobile except the windshield, the stress locked into the product depends on the rate at which the product is quenched in a final step. Hence there is a need for knowledge of the glass temperature at every step of the production process. In some cases, knowledge of the bulk temperature is sufficient. In others, such as during the tempering step, the needs become more specific. During the quenching process it is desirable to obtain both spatially and temporally resolved measurements of the temperature.

There has been considerable activity involving new and improved methods for measurement of glass temperature. Infrared sensors have shown promise for a non-contact method. An attempt to measure the temperature of a glass sheet at the top surface, middle, and back surface using an infrared radiometer in conjunction with numerical modeling demonstrated reasonable results [1]. However, some difficulties were noted for determination of the back surface temperature. The authors stated that the difficulty could be overcome by use of two radiometers viewing opposite surfaces of the samples. Other work involving a fiber optic temperature sensor has utilized a fluorescence intensity ratiometric method for temperature determination [2] and temperature and strain determination [3]. Direct measurements of fluorescence lifetimes in fiber optics have also been investigated over a number of years [4]. A comparison of the relative merits of both temperature sensor schemes has been made [5] in the case of fiber optics. It is clear that these methods could also be applied to glass products other than fibers. In many of these cases, the fibers were doped with neodymium or other rare-earth ions and the fluorescence resulting from the emissions from one or

---

[*] Corresponding Author. Tel.: +1-509-375-2438; fax: +1-509-375-6605.

E-mail address: moe.khaleel@pnl.gov (M.A. Khaleel).

0017-9310/01/$ - see front matter. Published by Elsevier Science Ltd.
PII: S0017-9310(01)00046-1

several rare-earth ion excited levels, whose populations were temperature sensitive, was recorded. Measurement of the fluorescence lifetime (from a single excited level) or of the ratios of the emission intensities (from two thermally coupled excited levels) allowed the determination of temperature, depending on the measurement scheme. Rare-earth-ion-doped fiber optic temperature sensors with very good sensitivities have been reported. In the case of an ytterbium doped fiber optic, an accuracy of approximately 1°C over the temperature range of 30–600°C was reported [6] while accuracies of about 3°C for temperatures between 0°C and 500°C were reported for neodymium doped fibers [2]. The method could be applicable to glass sheets, for example, if one used the trace amounts of neodymium naturally present in glass as the temperature-sensing element. However, rare-earth elements are typically present in raw materials at only about 1 part-per-million or less. Therefore the fluorescence emission from affected levels would most likely be too low to allow this method to be successful without active doping.

We have performed experiments with the goal of developing a method for measurement of temperature in glass products with the following features: (1) non-contacting, (2) real time, and (3) through-thickness.

The method that we describe below is based on fluorescence emission. Many glass products include Fe_2O_3 as an additive in various amounts. The transmission of the glass both within the ultraviolet (UV) range and in the infrared (IR) spectral range is affected by the iron ions present within the glass. In the case of automotive glass, it is desirable to reduce transmission of both of these bands in order to minimize damage to automotive interiors (UV) and to reduce the thermal load for air conditioning systems (IR). The absorption properties of both ferric and ferrous ions have been described in the literature [7,8]. It has been discovered in our work that absorption of light by iron ions in glass also results in a predictable fluorescence emission. The emission in turn depends on the glass temperature, and this dependence is the basis for our method of measuring temperature. We have measured the fluorescence emission lifetimes in several glass samples over a temperature range from 25°C to 550°C (about 300–825 K). Our research has shown that the method offers promise to fulfill the needs of the glass industry. However, improvements must be made in the temperature range of applicability and the temperature resolution.

The fluorescence method for measurement of temperature will be described in detail in the following sections of this paper. In Section 2 we will explain the basis for the method and describe the glass samples used in the experiments. In Section 3 we describe the experiments performed in the development of the method. The results will be presented in Section 4.

2. Description of the method

Typical soda-lime float glass is composed largely of SiO_2 (72% by weight), Na_2O (14%), CaO (9%), MgO (4%), and Fe_2O_3 (1%). The compositions vary somewhat depending on manufacturer and intended use, especially in the addition of other trace chemicals. Nominal compositions of three automotive glasses manufactured by Visteon Glass Division of Ford Motor Company are shown in Table 1. These glasses, termed Tint, Solar Tint, and Batch Privacy, are used as automotive windshields, sidelights, and backlights for Ford and other brands of vehicles. The experiments described later were performed largely with Tint, Solar Tint, and Batch Privacy samples. These samples were obtained (courtesy of Visteon) from standard production runs and thus the compositions are approximately as shown in Table 1. In addition, Visteon also made available glass samples of precisely known composition that were constructed under laboratory conditions with high purity materials.

In the wavelength range from about 300 to 1000 nm, light absorption in typical soda-lime float glass is largely due to either ferrous (Fe^{2+}) or ferric (Fe^{3+}) ions [8]. The absorption coefficients for Tint and Solar Tint glass are shown in Fig. 1. Note that there is a local maximum in the absorption coefficient near 380 nm. This peak has been shown to be due to absorption by ferric ions [8]. Hence, in the development of a temperature diagnostic based on fluorescence, this peak is a likely candidate for excitation.

In order to develop a fluorescence method for measurement of temperature, some preliminary experiments were performed to determine the absorption and emission properties of the glass samples. These experiments were performed with a SPEX spectrofluorometer. In one set of experiments, the samples were irradiated with light whose wavelength was scanned, while the emission was recorded at a fixed wavelength. In other experiments, the samples were irradiated at a fixed

Table 1
Nominal compositions (by weight) of Tint, Solar Tint, and Batch Privacy glass

	Tint	Solar Tint	Batch Privacy
SiO_2	72.23	72.45	71.6
Na_2O	13.6	13.69	13.7
CaO	8.75	8.44	8.45
MgO	3.89	3.55	3.5
Al_2O_3	0.6	0.6	0.6
Fe_2O_3	0.55	0.89	1.55
SO_3	0.24	0.22	0.18
K_2O	0.12	0.12	0.13
TiO_2	0.011	0.045	0.02
MnO_2	0	0	0.25
Se (ppm)	0	0	29
Co (ppm)	0	0	175
Total	99.991	100.005	99.98

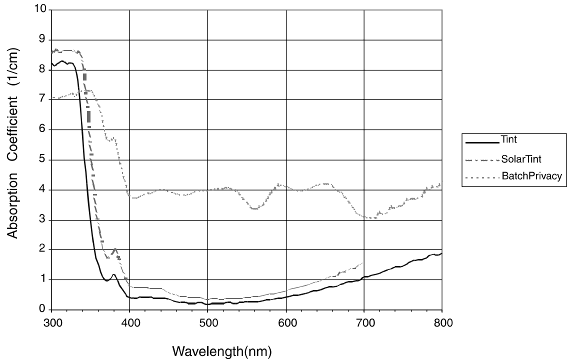

Fig. 1. Absorption coefficients for Tint, Solar Tint, and Batch Privacy glass as a function of temperature. Note the absorption peak at 380 nm.

wavelength while the wavelength of the detected emission was scanned and recorded. In both of these experiments, the excitation light source was continuous so that temporally resolved data were not obtained. These experiments have allowed some insight into the process by which fluorescence occurs in the glass samples.

The high purity samples had various concentrations of iron oxide, and the predominant ionic form of the iron was known since the production process was done under reducing, oxidizing, or neutral conditions. Under reducing conditions, production of ferrous (Fe^{2+}) ions is favored while under oxidizing conditions ferric (Fe^{3+}) ions are more readily produced. No actual quantitative information is known about the ratio of these species, however. The production methods for these samples are described in [7].

In Fig. 2, we show the emission at 670 nm while the excitation wavelength was scanned from 300 to 650 nm. Data for this plot were acquired with three high purity glass samples containing iron oxide at 0.2% by weight. The data show absorption peaks at 380, 425, and 450 nm. Note that 670 nm emission is strongest for the glass sample produced under oxidizing conditions, which presumably contains predominantly ferric ions. The sample produced under reducing conditions exhibits the least emission.

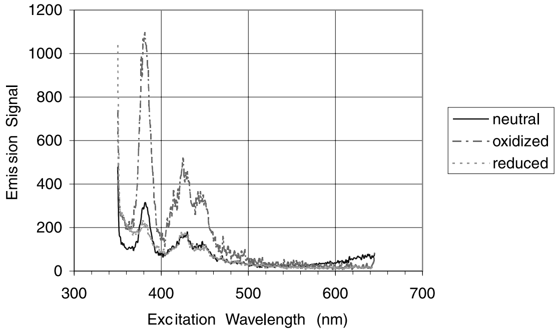

Fig. 2. Emission signal at 670 nm as a function of excitation wavelength for high purity glass samples.

In Fig. 3, we show the emission that results when the same three samples are irradiated at 380 nm. Note that emission from the reduced sample is strongest between 400 and 450 nm and there is relatively little emission at 670 nm. Emission at 670 nm is much stronger for the other two samples. Evaluation of a wide variety of data has not led to a consistent reason for the fluorescence difference, and the difference cannot clearly be correlated to the differences between ferrous and ferric ion concentration. It is more likely due to differences in the structure of the glass matrix. The data of Figs. 2 and 3 suggest that a fluorescence probe that utilizes either the emission at 450 or 670 nm may be useful if excitation is performed at about 380 nm. We chose to investigate the emission at 670 nm since additional early experiments showed that, at least qualitatively, the fluorescence signal depended on temperature. Future work will probe into the utility of the 450 nm emission as a possible fluorescence probe.

Utilizing the spectrofluorometer, we performed similar experiments with Tint, Solar Tint, and Batch Privacy samples. The resulting emissions observed when the samples were irradiated at 380 nm are shown in Fig. 4 for the Tint and Solar Tint samples. Note that the Tint sample shows fluorescence predominantly at 670 nm while the Solar Tint sample fluoresces mostly at 450 nm. All of these samples are produced under similar furnace conditions. The Tint and Solar Tint samples differ mostly in iron content (see Table 1).

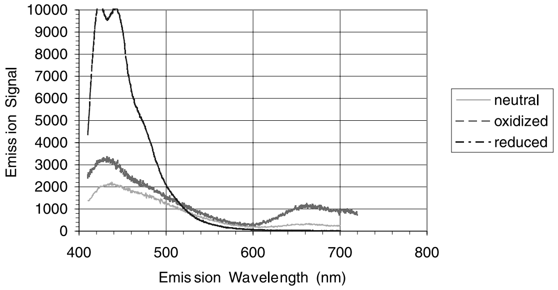

Fig. 3. Emission signal as a function of wavelength with fixed excitation at 380 nm. High purity glass samples were used in the measurements.

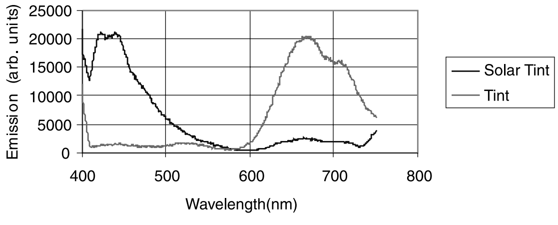

Fig. 4. Emission signal as a function of wavelength with fixed excitation at 380 nm. Data are shown for Tint and Solar Tint glass samples.

While absorption studies have shown that ferric and ferrous ions are mostly responsible for absorption in soda-lime glass, very little is known about the fluorescence emissions and the mechanisms ultimately responsible for them. The ferric ion is clearly very important for light absorption at 380 nm. Fluorescence quite likely depends on the glass matrix as well as the ionic form of the iron. Since the fluorescence spectra from the high purity samples and the batch samples are quite similar, it is not likely that other glass additives or impurities are responsible for the emission. Hence, many soda-lime glasses containing iron are very likely to exhibit the same general fluorescence observed in our experiments. However, it will probably always be necessary to test any individual type of soda-lime glass for its fluorescence behavior, since it may be that certain additives can suppress or quench fluorescence. For instance, we observe that the Batch Privacy sample, which is basically similar to the other glass samples except that it contains modest amounts of cobalt and significantly higher iron content, does not fluoresce with the same time signature as the other two samples and, additionally, does not fluoresce as strongly. The rare-earth element cerium is sometimes included as an additive in soda-lime glass, and this ion fluoresces strongly in the blue region of the light spectrum when excited by light of approximately 360 nm. Inclusion of significant amounts of cerium in a glass composition could be expected to make use of the iron fluorescence method of temperature determination very difficult.

The fluorescence from glass can be used as a temperature diagnostic if the fluorescence properties are related to the temperature in some manner. Following the preliminary experiments described above, we performed experiments to observe such behavior. A diagram of the experimental arrangement is shown in Fig. 5. A pulsed nitrogen laser was used to pump a dye laser, whose output was adjusted to 380 nm, through manipulations of the dye cell laser cavity. The dye laser light was directed by means of mirrors to a glass sample. Samples of Tint, Solar Tint, and Batch Privacy glass were tested. All samples were about 0.3 cm in thickness and 1.5 cm × 1.5 cm in cross-section. The light passed through the 0.3 cm thickness of glass at an angle of about 40° from the normal. After passing through the glass, the remaining laser light entered a beam dump drilled into the top of the oven. Fluorescence light originates and propagates from the small pencil-like region of glass through which the dye laser beam passed. A fraction of this light was collected with an optic and focused onto the plane of a segmented photomultiplier tube (PMT). The PMT has an active area of about 16 mm × 16 mm and is segmented into 16 channels, each channel being 1 mm × 16 mm in area. Since the fluorescence emission is imaged, light from various depths within the glass are focused onto various segments of the detector. We utilized three of the 16 segments, collecting fluorescence light emanating from near the top, middle, and bottom of the glass sample. The remaining 13 PMT channels were unused. Signals from each PMT channel first passed through a high gain current preamplifier before going to an oscilloscope for time resolved collection.

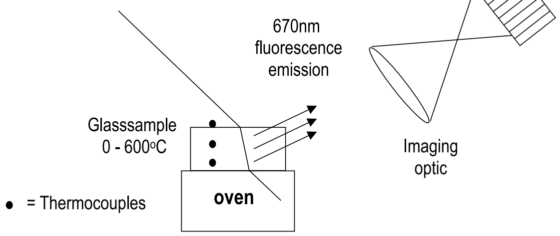

Fig. 5. Experimental arrangement for conducting fluorescence lifetime measurements in Tint, Solar Tint, and Batch Privacy glass samples.

The nitrogen laser coupled with the dye laser was used since no other convenient source of 380 nm laser light was available for these experiments. The dye laser pulse length was about 3 ns and the energy per pulse was about 50 μJ. The pulse repetition rate was 16/s. The dye used for the laser was BP-BD-365 which was manufactured by Exciton. The spectral width of the pulse was about 1 nm. No attempt was made to produce a beam of very narrow linewidth, since the glass absorption peak at 380 nm is quite broad and production of narrow linewidth beams invariably results in greatly reduced beam power.

The oven was constructed with a machinable ceramic body, and contained a coiled nichrome wire for a heating element. The wire was insulated from a stainless steel cover plate which rested above it with a thin sheet of mica. A 20 V–20 A DC power supply was used to provide power for heating the oven. At the highest temperatures, the electric power supplied was about 100 W. The oven was held on a standard optical rod affixed to a magnetic base, and the arrangement had sufficient flexibility to allow precise positioning of the oven in the optical scheme.

The glass samples were held flat against the stainless steel plate by a small leaf spring that covered only a small part of the sample. The glass samples were drilled through the sides to accept Type K chromel–alumel thermocouples. The drill holes were 0.5 mm in diameter and 0.5 cm in depth. One hole was placed at the bottom of the sample and another one was placed in the middle of the sample. A third thermocouple was placed on the top of the sample and attached with a high temperature ceramic epoxy. The drill holes extended to near the center of the samples. The glass samples were heated from the bottom. Heat loss from the samples was due to convection and conduction into the room air. No attempt was made to assure any particular thermal gradient within the sample. The thermocouples provided an independent measurement of glass sample temperature at three vertical positions. During experiments, the sample temperature was adjusted until a target temperature was reached for the center of the sample. Then all three temperatures were recorded and fluorescence measurements were obtained. Typically the temperatures could be controlled to within about 3°C of the target temperature during any single measurement.

The fluorescence light from the glass was imaged with an optical system consisting of a pair of lenses and light filters. The first lens was an $f/1$ plano-convex lens of 30 mm focal length. Separated from it by 43 mm was an achromatic doublet lens with a focal length of 40 mm. Both lenses featured axially varying refractive indices to reduce aberration. Filters were placed between the two lenses. These filters included two colored glass filters that passed light with wavelengths above 630 nm. Scattered laser light rejection was better than a factor of 10^6 with the colored glass filters. The photomultiplier response drops dramatically after 700 nm, so that the effective wavelength range of light collected was from 630 to 700 nm. The object distance was adjusted so that the image distance was about 15 cm behind the second lens and the image magnification was nearly three. Adjustment of the optical group to obtain the proper object and image distances was done by replacing the glass sample with a colored glass of nearly identical thickness and which exhibited strong fluorescence. The glass was irradiated with the dye laser beam and the fluorescence was sufficiently strong to easily obtain an image of the dye laser beam path through the glass. The detector position was adjusted so that imaged light from the top, middle, and bottom portions of the glass fell upon the correct segments of the PMT. The positions of the optics and detector were then fixed and an actual glass sample replaced the colored glass. Finally, a copper enclosure was built and installed around the optics, filters, detector, and preamplifier assembly in order to reduce interfering noise to an acceptable level. The noise was due to strong RF emission that resulted from operation of the nitrogen pump laser, which included a spark discharge.

3. Experimental procedure

The experimental arrangement is shown in Fig. 5. A glass sample was placed on top of the oven and held in contact with the oven surface by means of a steel spring. The thermocouples were inserted into the samples and each thermocouple was connected to a readout instrument. Laser light from the dye cell was then directed onto the glass sample and the light emission at wavelengths longer than 630 nm was recorded on three channels of the 16 channel PMT. The output signals from the PMT ran first through a current preamplifier with a gain of 5×10^4 V/A before going to the input terminal of a four channel digital oscilloscope. Oscilloscope triggering was provided by a photodiode which sampled scattered laser light. For each laser shot, the time resolved signal from each of the three PMT channels was recorded. Each recorded spectrum was an average of 200 laser shots. Typical recording time for one spectrum was about 1 min. This recording time was convenient for experimental purposes. However, in actual use of a perfected instrument in a plant setting, the integration time will need to be reduced to about 1 s in order to observe fast thermal transients associated with thermal quenching of tempered products. This time requirement will translate into the need for a much higher power laser (for instance, a pulsed, frequency doubled Alexandrite laser) operating at an improved repetition rate. The data were stored in the oscilloscope memory buffers and then subsequently transferred to a dedicated PC for storage in data files. Data were recorded with 16-bit precision. An experiment would begin with the glass sample at room temperature. After collection of data, the temperature of the oven would be increased to predetermined levels beginning at 50°C and increasing by 50°C for each subsequent measurement. The final temperature was typically around 550°C. Then data would be recorded as the temperature was decreased from 500°C to 100°C in 50°C increments. The glass temperatures as recorded with the thermocouples typically varied by about 3°C during each measurement. The average temperature for each thermocouple was recorded with each data set. As expected, a thermal gradient existed within any tested glass sample, with the bottom of the sample being warmer than the top. The gradient increased with increasing average temperature.

Typical spectra obtained for the Solar Tint sample at 100°C, 200°C, and 300°C are shown in Fig. 6. The red fluorescence is seen to have a persistence time which decreases with increasing temperature. The magnitude (peak signal) of the fluorescence is also seen to diminish with increasing temperature. The initial signal is believed to be due to a prompt fluorescence emission. This signal has a full width at half maximum of about 10 ns (consistent with the system bandwidth of 100 MHz), and is fairly constant in amplitude over the experimental range of temperatures. Inclusion of additional filtering to increase rejection of dye laser light did not appreciably alter this signal, and therefore we have concluded that the signal is not due to scattered laser light. Since this signal has only modest temperature dependence, at least in amplitude, no useful purpose can be made of it in these experiments. In the determinations of lifetimes, analysis excluded the region in time occupied by the initial pulse.

If we define the fluorescence lifetime as the time required for the signal to fall from its peak value above

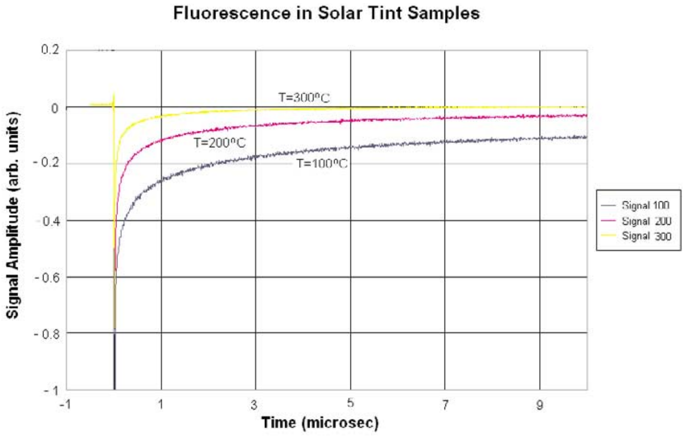

Fig. 6. Time resolved fluorescence spectra obtained at several temperatures for a Solar Tint glass sample. Both the fluorescence signal and the fluorescence lifetime decrease with increasing temperature.

baseline to $1/e$ of its value above baseline then we can determine fluorescence lifetime as a function of temperature from plots such as shown in Fig. 6. A plot of fluorescence lifetime as a function of temperature is shown in Fig. 7 for the Solar Tint glass sample.

Detailed knowledge of the fluorescence process in iron-doped glass samples is not presently well known. There has been research performed to study the emission from rare-earth ions in glasses and crystals, where the 4f electrons of trivalent rare earths are only weakly coupled to their environments through the crystal fields of the surrounding ions [9–11]. For most other ions, such as iron, the coupling of an excited electronic state to the crystal field should be much stronger. The observed fluorescence is most likely due to the existence of a collective state formed by the iron ions and the surrounding glass matrix. Optical absorption and emission lines are very broad, due to coupling between collective states and the crystal fields, which vary spatially. Not surprisingly, the observed fluorescence emission decay is not truly exponential in time, as has been noted in other studies [9]. In most cases, however, a single exponential curve represents most of the data reasonably closely. In the case of ions other than the rare earths, the mechanisms for light absorption and emission are very poorly known.

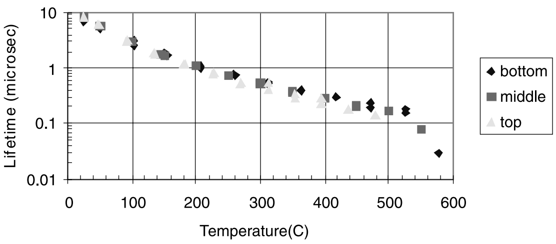

Fig. 7. Plot of fluorescence lifetime as a function of temperature for a Solar Tint glass sample.

It is beyond the scope of this research to address detailed questions of absorption and emission of light by iron-doped glass. The main purpose of our study is to demonstrate that the observed phenomena can be used as a temperature diagnostic. However, an extremely simplified model can be constructed and tested against the data. Upon absorption of light by a ferric ion in a glass matrix, the energy must be dissipated in some manner. Competing channels include radiative and radiationless transitions to other energy states. Radiationless transitions occur through coupling of the excited state to the phonon field of the surrounding lattice. With increasing temperatures, radiationless transitions become more important as the occupation number of high-energy phonon modes increases. It is possible for phonons to result in a transition to either a higher or lower energy state. The subsequent decays from these other states are not observed with our instrumentation. Since we observe only radiative transitions at about 670 nm, the emitted light diminishes with increasing temperature and the fluorescence lifetime also becomes shorter.

The temperature dependence of the fluorescence lifetime will depend on the mechanism by which the relevant excited states become de-populated. There are probably a multitude of non-radiative transitions that could be mediated in the glass in a way that produces the observed temperature dependence, and it is not possible to arrive at a most likely mechanism from the data at hand. With this disclaimer, the simplest mechanism has been considered: the excited state formed by absorption of light at 380 nm interacts with the phonon field to transition to either a higher or lower energy state by absorption or emission of a phonon. The new excited state then would decay unobserved to the ground state or another lower energy state. In this model the fluorescence emission at 670 nm would diminish since the population of fluorescing states becomes depleted due to interaction with the phonon field. For such a process the transition rate will depend directly on the occupation number for the phonon mode, which, for phonon energies much larger than kT is given by

$$n(T) = \exp(-hv/kT), \tag{1}$$

where h is Planck's constant, v is the frequency, k is Boltzmann's constant, and T is the Kelvin temperature.

Hence the transition rate, R, which is proportional to the phonon occupation number, is given by

$$R = R_0 \exp\left(\frac{-E_a}{kT}\right), \tag{2}$$

where E_a is the activation energy which must be thermally supplied and R_0 is a constant of proportionality. The excited state is then de-populated by phonon interaction and by radiative decay. We assume that the radiative decay rate from the initial excited state is much smaller than the rate at which phonons de-populate the state, so that the phonon rate alone adequately describes the process. Since R is inversely proportional to the lifetime τ we obtain after some manipulation

$$\ln \tau = \ln \tau_0 + \frac{E_\alpha}{kT}. \tag{3}$$

Thus, a plot of $\log \tau$ vs $(1/T)$ should yield a straight line with slope (E_a/k). The data are plotted as described for the Solar Tint sample in Fig. 8. The line slope gives $E_a = 2.7 \times 10^{-20}$ J (0.17 eV). Similar data for Tint and Batch Privacy glass samples provide $E_a = 2.3 \times 10^{-20}$ J (0.15 eV) and $E_a = 7.7 \times 10^{-21}$ J (0.05 eV) for Tint and Batch Privacy glass, respectively. For oxide glasses, the energies of the highest frequency vibrations correspond to phonon energies in the range from 0.09 to 0.17 eV [9], so that the activation energies are fairly consistent with the energies available from single phonons in typical glasses. It is seen that the experimental fluorescence data are consistent with this simplified mechanism. As mentioned above, many other mechanisms may also lead to predictions that are reasonably consistent with the data. One such mechanism is multiphonon decay, where transitions between excited electronic states are facilitated through interactions with several phonons. Such a process adequately describes fluorescence lifetimes of rare-earth ions in glass [9–11]. For certain rare-earth ions, the electronic states are known, and estimates of the number of phonons necessary to facilitate a transition can be made. However, in the case of Fe_2O_3 in glass this mechanism cannot presently be tested since the existence of other electronic states has not been established. There is no means to assess the energy gap between excited states and obtain the corresponding number of phonons necessary to bridge this gap, if indeed such a gap exists.

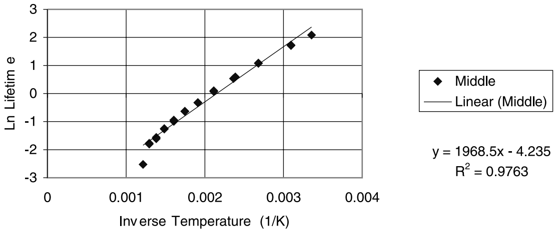

Fig. 8. Plot of the logarithm of the fluorescence lifetime against inverse Kelvin temperature for a Solar Tint glass sample. A best-fit linear plot, expected based on a simple model, is included with the data.

4. Results and discussion

Plots of the fluorescence lifetimes as a function of inverse temperature are shown in Fig. 9 for Tint, Solar Tint, and Batch Privacy glass samples. Several observations can be made from the plots. All three samples follow different curves, and thus the use of this method would require separate calibrations for each glass type. The Tint and Solar Tint samples show only minor differences. The Batch privacy sample shows a change of only about a factor of 10 in fluorescence lifetime over the experimental temperature range. It is doubtful that this method can be successfully used with such a dark, highly absorbing glass. For the other two samples, the experimentally useful temperature range is from about 20°C to 500°C. It is important that any method be able to reliably determine temperatures between about 200°C and 600°C (near the softening point of automotive glass). Above 500°C, system noise is sufficient to make temperature determination unreliable. However, the main noise source in our case was blackbody emission from the heated oven surface. This noise is very efficiently collected by the imaging optic. Light collected by the PMT was of wavelengths between 630 nm (lower limit of high pass color filter) and about 700 nm (cutoff of PMT response). A narrow band interference filter may have helped in noise reduction but such a filter would have also resulted in significant signal loss since the fluorescence has a broad frequency range. In actual

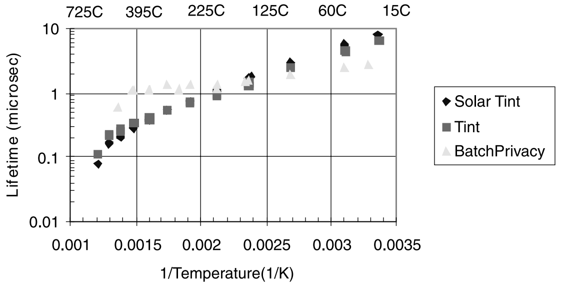

Fig. 9. Logarithmic plot of the fluorescence lifetime as a function of inverse Kelvin temperature for Tint, Solar Tint, and Batch Privacy glass.

field use, this noise may not be present. Thus the operational range of such a diagnostic may be increased if background noise can be significantly reduced. Future experiments will utilize a more efficient method for heating the glass with a reduction in background noise.

Even if background noise can be controlled or mitigated there will still be some fundamental limit to the attainable precision of the method. Taking the derivative of Eq. (3) we obtain

$$\frac{\mathrm{d}\tau}{\tau} = \frac{E_\alpha}{k}\frac{\mathrm{d}T}{T^2}. \tag{4}$$

Therefore, if Eq. (3) is a reasonably close approximation of the dependence of fluorescence lifetime on temperature, we can roughly estimate the precision with which we can measure temperature from Eq. (4). If we assume that lifetimes can be measured to within an accuracy of 1% and use $E_a = 0.17$ eV and $k = 8.6 \times 10^{-5}$ eV/ K then the precision with which we can determine temperature can be calculated. At a temperature of 300 K we obtain $\delta T = 0.5$ K. For 900 K we obtain $\delta T = 4.1$ K. These uncertainties are sufficiently small for the method to be viable in glass industry applications.

From the data presented in Figs. 7–9, it is clear that the achieved precision falls significantly short of the values calculated from Eq. (4). Based on the observed scatter in the data, we estimate that the temperature uncertainty at 300 K is about 2 K while at 800 K the uncertainty is about 35 K. There are several contributing factors to the enhanced uncertainties present in the data. Firstly, we are not able to determine lifetimes to within 1%. The deviation from a best fit curve of the lifetimes observed in multiple experiments is about 3% at 300 K and about 11% at 800 K. Several factors account for this variation, including poor counting statistics, electronic noise, background radiation noise at high temperatures, and unstable dye laser operation. This problem could largely be addressed with a better laser source, and tunable solid state lasers are now available that will provide much higher pulse energy at the desired wavelength. For instance, a pulsed Alexandrite laser can supply light at the appropriate wavelength with pulse energies 1000 times that available in this experiment. Efforts need to be made to reduce the background thermal radiation at high temperatures. Remote heating of the samples to the desired temperatures can help achieve a significant reduction in background signal. Another problem is caused by the prompt emission from the glass. This light is detrimental to the performance of the PMT since it depletes the electrons needed for amplification, resulting in gain nonlinearities. A gated version of the PMT is needed to enhance measurement performance. Subsequent research will address these issues. By inclusion of a pulsed Alexandrite laser, background signal reduction, and gating of the PMT, it is presently estimated that the measurement method can be improved sufficiently to allow temperature determinations up to about 600°C with a resolution of about 5°C and with a measurement time of 1 s.

Acknowledgements

DOE, under the Office of Industrial Technology, provided financial support for this project, while Visteon Glass Division of Ford Motor Company provided matching in-kind support. The authors are grateful for the help and encouragement provided by Mr. Theo Johnson of DOE-OIT. The authors wish to thank Mr. V. Henry, Dr. K.K. Koram, Dr. J. Haywood, and Dr. E. Boulos, all of Visteon Glass Division, for their help and contributions towards this effort.

References

[1] D. Mann, R. Viskanta, An inverse method for determining transient temperature distribution in glass plate, Inverse Problems Eng. 1 (1995) 273.

[2] S.A. Wade, J.C. Muscat, S.F. Collins, G.W. Baxter, Nd^{3+}-doped optical fiber temperature sensor using the fluorescence intensity ratio technique, Rev. Sci. Instr. 70 (1999) 4279.

[3] S.A. Wade, G.W. Baxter, S.F. Collins, K.T.V. Grattan, T. Sun, Simultaneous strain–temperature measurement using fluorescence from Yb-doped silica fiber, Rev. Sci. Instr. 71 (2000) 2267.

[4] K.T.V. Grattan, Z.Y. Zhang, Fiber Optic Fluorescence Thermometry, Chapman & Hall, London, 1995.

[5] S.F. Collins, G.W. Baxter, S.A. Wade, T. Sun, K.T.V. Grattan, Z.Y. Zhang, A.W. Palmer, Comparison of fluorescence-based temperature sensor schemes: theoretical analysis and experimental verification, J. Appl. Phys. 84 (1998) 4649.

[6] E. Maurice, S.A. Wade, S.F. Collins, G. Monnom, G.W. Baxter, Self-referenced point temperature sensor based on a fluorescence intensity ratio in Yb^{3+}-doped silica fiber, Appl. Opt. 36 (1997) 8264.

[7] E.N. Boulos, L.B. Glebov, T.V. Smirnova, Absorption of iron and water in the Na_2O–CaO–MgO–SiO_2 glasses: part 1: separation of ferrous and hydroxyl spectra in the near IR region, J. Non-Cryst. Solids 221 (1997) 213–221.

[8] L.B. Glebov, E.N. Boulos, Absorption of iron and water in the Na_2O–CaO–MgO–SiO_2 glasses: part 2: selection of intrinsic, ferric and ferrous spectra in the visible and UV regions, J. Non-Cryst. Solids 242 (1998) 49–62.

[9] C.B. Layne, W.H. Lowdermilk, M.J. Weber, Muliphonon relaxation of rare-earth ions in oxide glasses, Rhys. Rev. B 16 (1977) 10.

[10] L.A. Riseberg, H.W. Moos, Multiphonon orbit-lattice relaxation of rare-earth ions in crystals, Phys. Rev. 174 (1968) 429.

[11] M.J. Weber, Radiative and multiphonon relaxation of rare-earth ions in Y_2O_3, Phys. Rev. 171 (1968) 283.